MANSOURA JOURNAL OF CHEMISTRY
Official Journal of Faculty of Science, Mansoura University, Egypt
E-mail: scimag@mans.edu.eg ISSN: 2974-4938

Evaluation of Electrochemical Behavior of $CuCl_2$ in Absences/Presences of 3-(2-(4-aminobenzoyl) hydrazono)-N-(pyridin-2-yl) butanamide: Cyclic Voltammetric and Tafel Slopes Evaluation

L. A Yasin[1], M. Gaber[1], K. Y El-Baradie[1], E. A Gomaa[2], R. R. Zaky*[2]

[1]Chemistry Department, Faculty of Science, Tanta University, Egypt

[2]Chemistry Department, Faculty of Science, Mansoura University, Egypt

**** Correspondence to:** Rania R. Zaky, Department of Chemistry, Faculty of Science, Mansoura University, Mansoura, Egypt, E-mail; rania.zaky@yahoo.com, Tel: 00201097799452*

Received:12/06/2024
Accepted: 08/07/2024

Abstract: The electrochemical behavior of $CuCl_2$ in a 0.1 M KCl solution was investigated using cyclic voltammetry, employing a conventional glassy carbon electrode in conjunction with an Ag/AgCl reference electrode. At nearby (1.0 -1.5)V, two prominent reduction and two oxidation peaks were recognized. Upon increasing the concentrations of $CuCl_2$, both the cathodic and oxidation waves were greater than before, indicating a direct correlation between cupric chloride concentration and the observed electrochemical responses. The recorded peaks signify the transition from divalent to monovalent copper ions, occurring within the reduction process .Conversely, during the oxidation process, the reverse oxidation occurs, converting the monovalent copper ions back to their divalent state. Subsequently, the solvation thermodynamic properties were evaluated and discussed. Additionally, the complexation reaction between $CuCl_2$ and 3-(2-(4-aminobenzoyl) hydrazono)-N-(pyridin-2-yl) butanamide (H_2ABHPB) ligand, was studied. The Gibbs free energies associated with the interaction of CuCl2 with the employed ligand (H_2ABHPB) were determined and found to be within 48 to 50.8 kJ/mol range, proving strong interaction. Subsequent, analysis involved the estimation of Tafel slopes for the electrochemical in absence/presence ligand H_2ABHPB were studied. This investigation revealed the coexistence of diffusion-controlled electron transfer and mass transfer mechanisms. Furthermore, the Tafel equation parameters were scrutinized to gain insights into the underlying electrochemical processes.

keywords: Cyclic voltammetry, solvation parameters, thermodynamic parameters, Tafel slopes, Stability constants

1.Introduction

During cyclic voltammetry experiments conducted with cupric chloride, various features become apparent in the voltammogram [1, 2]. Initially, at more negative potentials, the reduction of cupric chloride can take place, thereby resulting in the formation of cuprous chloride [3-6]. This reduction process is frequently identified by a reduction peak or wave, indicating the conversion of Cu(II) to Cu(I). As the potential progressively shifts towards more positive values, the reverse process occurs, with cuprous chloride oxidizing back to cupric chloride, thereby manifesting an oxidation peak or wave within the voltammogram [7-11]. The position, shape, and intensity of these peaks yield valuable insights into the kinetics and thermodynamics governing the redox reaction associated with cupric chloride [12-16]. It's noteworthy that the specific features observed in the cyclic voltammogram of cupric chloride can be influenced by various factors such as scan rate, supporting electrolyte, pH, and electrode material. Optimization of these experimental parameters is crucial for enhancing the detection and characterization of cupric chloride in cyclic voltammetry investigations [17-20].

Cupric chloride finds diverse applications across multiple industries. Firstly, in electroplating, it serves as an electrolyte essential for copper deposition, ensuring the creation of uniform and adherent copper coatings on various substrates [21]. Secondly, cupric chloride acts as a

catalyst in numerous organic chemistry syntheses, owing to its catalytic properties. Thirdly, it serves as a pigment, imparting blue and green hues, making it valuable in coloring applications [22]. Fourthly, cupric chloride serves as an etching solution for metals like copper, brass, and bronze, facilitating precise metal etching processes [23]. Lastly, it plays a crucial role in gas scrubbers, where it reacts with hydrogen sulfide in industrial gases to form copper sulfide precipitates, thereby aiding in the removal of harmful pollutants [24]. These are few examples of the uses of cupric chloride and its application which must followed cyclic voltammetrically. Based on the above, we study the electrochemical behavior of $CuCl_2$ in Absences/Presences of 3-(2-(4-aminobenzoyl) hydrazono)-N-(pyridin-2-yl) butanamide using cyclic voltammetry. This study demonstrated the determination of the stochiometric ratios for the association of Cu ions with ligand in the solution by plotting molar ratio (j) which were obtained *via* adding the (H_2ABHPB) ligand to the solution of Cu(II) ions versus (ip,a or ΔE°). As a result, we studied the complexation interaction between Cu(II) ions and ligand and identified the complex forms in the solution and calculated the stability constants and Gibbs free energies for these complex forms. Finally, we studied the complexation effects on the system reversibility degree and compared them to the electrochemical behavior of free Cu(II) ions as a reference.

2. Experimental

In this study, $CuCl_2.2H_2O$, DMSO, and KCl were used without any treatment, and they were provided by Sigma-Aldrich and Merck. The DY2000 (USA) apparatus was utilized to perform cyclic voltammetry. measurements, employing a sophisticated three-electrode configuration as shown in Figure 1. The auxiliary electrode utilized was a platinum electrode, while the reference electrode was Ag/AgCl/saturated KCl. The working electrode employed was a glassy carbon electrode. A study of the electrochemical behavior of Cu(II) ions at 291.45 K had been conducted using 0.1 M of KCl solution as the supporting electrolyte dissolved in 50 % (DMSO-water) mixed solvent. To study the electrochemical behavior of the H_2ABHPB ligand Structure 1, all cyclic voltammograms were recorded according to the IUPAC convention at 297 K.

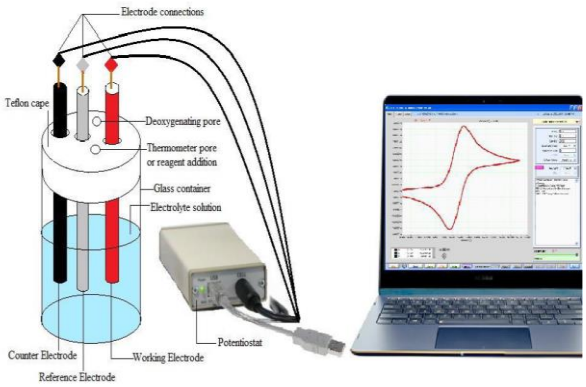

Figure 1. The Electrochemical setup

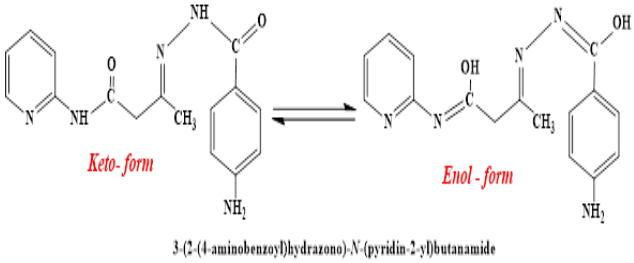

Structure 1. Ligand H_2ABHPB

3. Results and Discussion

3.1.Cupric ion cyclic voltammetry

In the cyclic voltammetry analysis of a 0.1M KCl solution, various concentrations of cupric chloride (0.1M) were introduced using a glassy carbon working electrode. Notably, the addition of the cupric chloride resulted in observable waves, particularly in the presence of a gold electrode. At around 1.0V and -1.5V, two prominent reduction and two oxidation peaks were identified. Upon increasing the concentrations of $CuCl_2$, both the cathodic and oxidation waves were augmented, indicating a direct correlation between cupric chloride concentration and the observed electrochemical responses. We concentrate in this work on the transfer of cupric ion to cuprous one. This is illustrated by the first reduction wave and its reverse first oxidation peak as seen in Figure 2. The recorded peaks signify the transition from divalent to monovalent copper ions, occurring within the reduction process .

Conversely, during the oxidation process, the reverse oxidation occurs, converting the monovalent copper ions back to their divalent state.

Table (1): Effect of different concentrations of copper chloride at 291.45 K with a scan rate 0.1 V/s

[M] x10^{-3} mol/L	Ep,c V	Ep,a V	ΔEp V	(-) Ip,a µA	Ip,c µA	Ip,a/Ip,c	E° V	Dc x10^{-6} cm^2.s^{-1}	Da x10^{-6} cm^2.s^{-1}	α_{nac}	ksc cm/s	Γ a x10-8 mol.cm-2	(-) Qa x10^{-4} C	Γ c x10^{-8} mol.cm-2	(+) Qc x10^{-4} C
1.64	-0.06	0.051	0.111	0.07	22.4	0.313	-0.004	3.27	32.19	1.084	0.74	0.058	0.04	0.185	0.11
3.23	-0.035	0.101	0.136	118	53.1	2.218	0.033	4.75	23.40	1.059	1.46	0.977	0.59	0.440	0.26
4.76	-0.077	0.121	0.198	168	90.3	1.854	0.022	6.30	21.69	0.547	4.16	1.388	0.84	0.748	0.45
6.25	-0.066	0.139	0.205	234	110	2.134	0.036	5.38	24.51	0.696	4.99	1.938	1.17	0.907	0.55
7.69	-0.078	0.153	0.231	304	118	2.586	0.037	4.09	27.39	0.575	6.64	2.521	1.53	0.974	0.59

Table (2): Effect of different scan rates of 7.69 x 10-3 M copper chloride at 291.45 K

ν V/s	Ep,c V	Ep,a V	ΔEp V	(-)Ip,a µA	Ip,c µA	Ip,a/Ip,c	E° V	Dc x10-3 cm2.s-1	Da x10-3 cm2.s-1	αna	ksc	Γ a x10^{-8} mol. cm^{-2}	(-)Qa x10^{-4}C	Γ c x10^{-8} mol.cm-2	(+)Qc x10^{-4}C
0.1	-0.078	0.153	0.231	304	118	2.587	0.038	0.409	2.74	0.576	6.64	2.521	1.53	0.975	0.59
0.05	-0.095	0.139	0.234	255	92.2	2.764	0.022	0.504	3.85	0.508	5.19	4.226	2.56	1.528	0.93
0.02	-0.048	0.127	0.175	224	58.1	3.856	0.039	0.499	7.42	0.630	1.12	9.281	5.62	2.407	1.46
0.01	-0.049	0.124	0.173	196	48.0	4.082	0.037	0.683	11.4	0.630	0.89	16.246	9.84	3.980	2.41

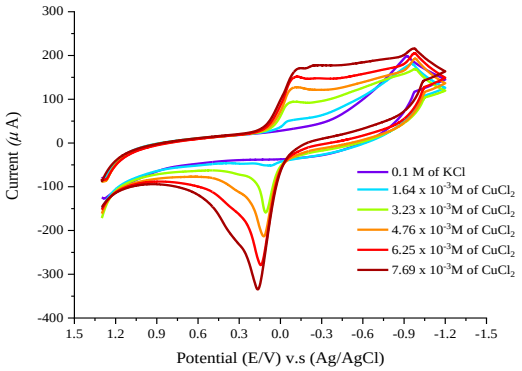

Figure 2. Effect of different concentrations of $CuCl_2$ at 291.45 K with a scan rate 0.1 V/s

The solvation and kinetic characteristics of $CuCl_2$ in a 0.1 M KCl solution at 291.45 K were assessed utilizing a glassy carbon working electrode. These evaluations were conducted following the methodologies outlined in prior studies [25-30], and the resultant values were tabulated in the Tables (1&2). Remarkably, the majority of the data was showcased within these tables exhibited an increase corresponding to higher concentrations of $CuCl_2$, suggesting a diffusion mechanism underlying the observed trends.

The impact of scan rates was investigated in a 0.1 M KCl solution employing a glassy carbon working electrode, with the resultant cyclic voltammograms depicted in Figure 3. Accompanying analysis data can be found in Table 2. It is noteworthy that most of the data exhibit a decrease with decreasing scan rates, suggesting the involvement of a diffusion mechanism. Furthermore, it is observed that the electron transfer rate constant is a substantial value, indicative of the rapid transfer of cupric ions to cuprous ions. The study involved examining the cyclic voltammetry of CuCl2 in a solution containing (0.1 M) KCl, while incorporating varying concentrations of the prepared ligand.

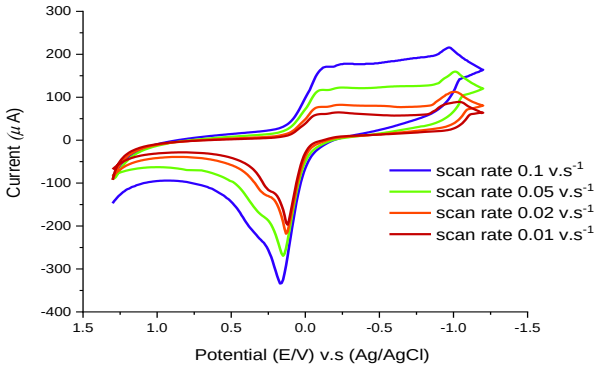

Figure 3. Effect of different scan rates of 7.69 x 10^{-3} M $CuCl_2$ at 291.45 K

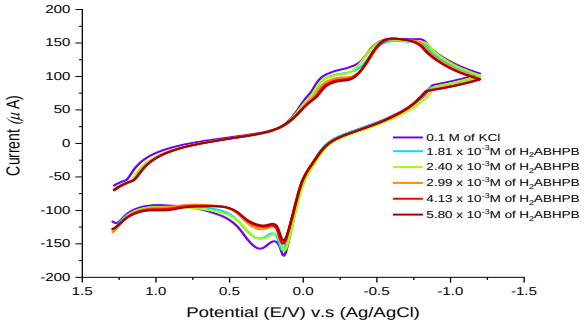

Figure 4. Effect of different concentrations of ligand H_2ABHPB at 291.45 K with a scan rate 0.1 V/s

Table (3): Effect of different concentrations of ligand H_2ABHPB at 291.45 K with a scan rate 0.1 V/s

[M] x10-3 mol/L	[L] x10-3 mol/L	Ep,c V	Ep,a V	ΔEp V	(-)Ip,a µA	Ip,c µA	Ip,a/Ip,c	E° V	Dc x10^{-6} $cm^2.s^{-1}$	Da x10^{-6} $cm^2.s^{-1}$	αna	ksc cm/s	Γ a x10^{-8} $mol.cm^{-2}$	(-) Qa x10^{-4} C	Γ c x10^{-8} $mol.cm^{-2}$	(+)Qc x10^{-4} C
7.55	1.81	0.129	-0.56	-0.689	32.7	-143	-0.229	-0.21	12.5	0.657	-0.576	9.10	0.542	0.329	2.365	1.43
7.51	2.40	0.124	-0.57	-0.694	39.1	-134	-0.292	-0.22	11.1	0.952	-0.639	8.19	0.649	0.393	2.218	1.34
7.46	2.99	0.127	-0.56	-0.687	39.0	-129	-0.303	-0.21	10.4	0.957	-0.568	8.58	0.647	0.392	2.131	1.29
7.37	4.13	0.129	-0.55	-0.679	37.1	-133	-0.279	-0.21	11.3	0.887	-0.576	10.6	0.615	0.373	2.196	1.33
7.29	5.25	0.122	-0.59	-0.712	46.7	-119	-0.392	-0.23	9.44	1.456	0.156	2.61	0.774	0.469	1.972	1.20

According to Figure 4 the analysis solvation parameters were evaluated from the cyclic voltammograms following different equations as given in literature [25-35] and presented in Table 3. The electron transfer rate constant for $CuCl_2$+ ligand [H_2ABHPB] solution is greater than that in presence of $CuCl_2$ alone indicating formation of cuprous complex with [H_2ABHPB] by the interaction between metal cupric solution and ligand used.

Table (4): Stability constant for (Cu-ligand) complex

(E°) M V	(E°) C V	(ΔE) V	J ($L.M^{-1}$)	(log βj)	(ΔG) kJ mol^{-1}
0.022	-0.2155	0.2375	0.024	8.3678	-46.3277
0.022	-0.223	0.245	0.032	8.6552	-47.9190
0.022	-0.2165	0.2385	0.04	8.45390	-46.8041
0.022	-0.2105	0.2325	0.056	8.2653	-45.9184
0.022	-0.2235	0.2455	0.072	8.7342	-48.6908
0.022	-0.234	0.256	0.08	9.0901	-50.8489

3.1.Analyzing Tafel plot

In Figure 1S, distinct linear relationships were depicted in the Tafel plots, illustrating the connection between over voltage, the measured volt and logarithm of peak current during the ascending phase of the cupric to cuprous reduction peak. This correlation was observed across varying $CuCl_2$ concentrations, both in absence and in presence of the ligand [H_2ABHPB]. Each plot represented a unique scenario, showcasing the nuanced interplay between these parameters under different experimental conditions. The Tafel plots appeared two straight lines for $CuCl_2$ alone with slopes equal to 0.615 and 0.5, respectively. The first line had large Tafel slope greater than the second indicating catalytic reaction appeared, whereas the second portion indicated diffusion-controlled reaction. Tafel plot for the effect of different concentrations from ligand [H_2ABHPB] on the cuprous ion peak gave three different jointed straight lines with slopes of 0.123, 0.5 and 0.2654, respectively. The mechanism of reaction $CuCl_2$ + [H_2ABHPB] according to Tafel plots are kinetic, diffusion and kinetic. The first kinetic reaction was corresponding to electron transfer reaction [34, 35]. Tafel equation, acting as a simplified model, allows for the extraction of essential parameters from electrochemical systems. These parameters included exchange current densities and Tafel slopes, providing valuable insights into the underlying processes of the system [36].The diffusion reaction was corresponding to mass transfer for cupric to cuprous ions vial diffusion and concentration mechanism. Lastly was the fast-kinetic reduction of cuprous to Cu zero charge.

The intercept plot value is greater for the two straight lines in $CuCl_2$+[H_2ABHPB] than that of $CuCl_2$ alone indicating complex reaction between the two materials. On studying the diffusion process in the reduction of copper ions in absence and presence of the used ligand, alpha the reversibility degree calculated from the Tafel slopes (Figures 1S & 2S) are almost the same in Tafel plot relation analysis for different concentrations of copper salt alone. On adding the ligand to the copper salt used the alpha parameter obtained from the Tafel plot slope are decreased in comparison to the salt alone indicating decrease of the reversibility of reaction due to the complexation character and more decreased by increase of ligand concentration.

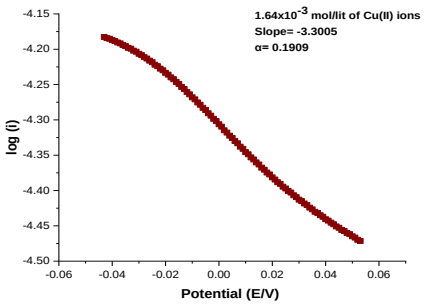

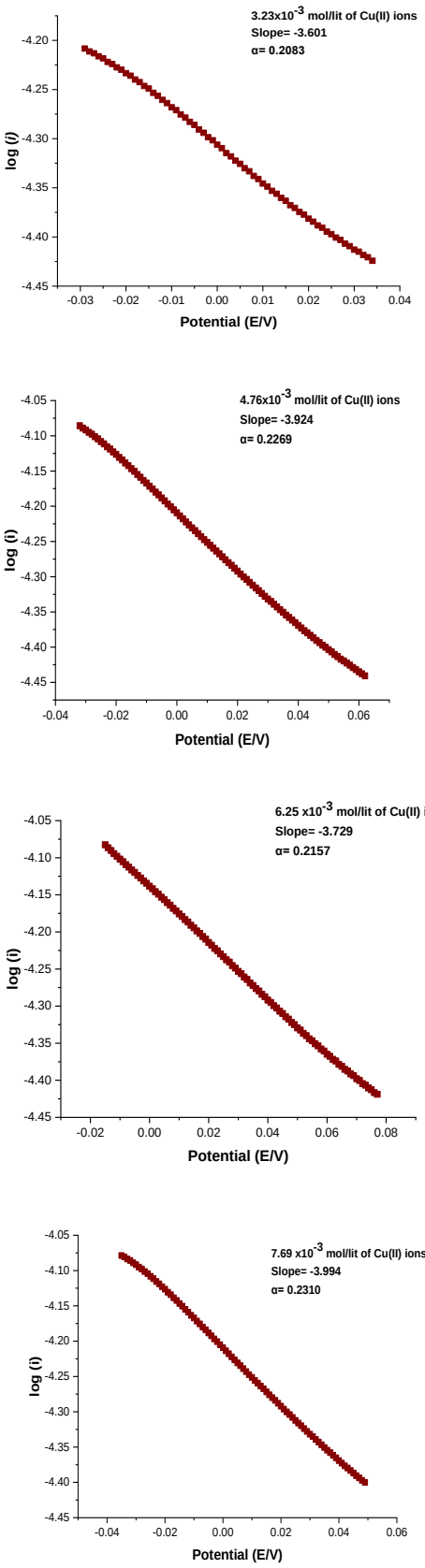

Fig. 1S Tafel plot for different concentrations of Cu(II) ions.

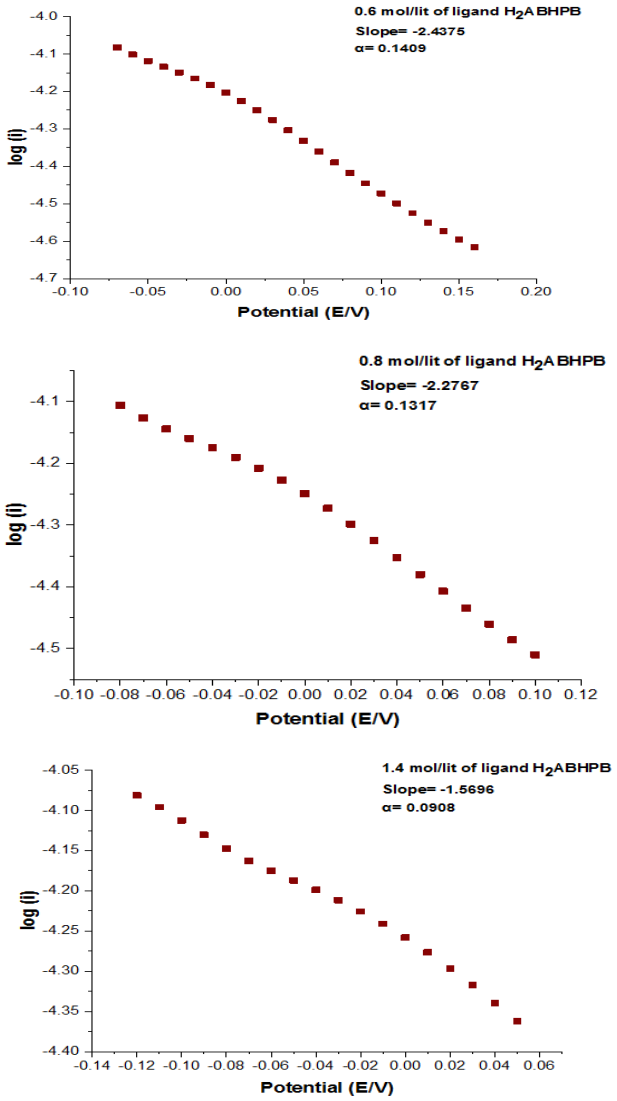

Fig. 2S Tafel plot for different concentrations of ligand H_2ABHPB.

3.2.Exploring the Gibbs free energies associated with the interaction between $CuCl_2$ and [H_2ABHPB] in a solution containing 0.1 M KCl.

Based on the references cited [28-37], The stability constants and Gibbs free energies which related to the interaction between CuCl2 and [H_2ABHPB] were examined and evaluated. The resulting values are presented in Table 4. Notably, the Gibbs free energies fall within a range typically observed between chemical and physical processes, indicating a significant degree of interatomic complexation rather than mere hydrogen bonding. This underscores the substantial nature of the interactions between the species involved. In continuation to our previous works [20, 22, 28] this work is done to illustrate and gave more light on solvation in solutions.

4. C onclutions

In this subsequent inquiry, building upon prior investigations, the quantification of cupric and cuprous ions is facilitated through cyclic voltammetry, utilizing a glassy carbon working electrode. The impact of varying concentrations of the ligand [H_2ABHPB] is examined, with thorough scrutiny applied to kinetic, solvation, and thermodynamic parameters, their implications thoughtfully deliberated. Notably, our analysis reveals novel insights into the electrochemical behavior of the Cu-H_2ABHPB system .

Tafel plots are meticulously constructed to illustrate reduction potentials, delineating the correlation between overvoltage and the logarithm of current for both the Cuprous peak and the $CuCl_2$ + [H_2ABHPB] ligand complex, yielding distinct linear relationships. The slopes derived from these Tafel plots are analyzed, providing insights into the electrochemical mechanism's operative, suggesting a confluence of kinetic and diffusion phenomena within the scrutinized medium.

This investigation uniquely elucidates the dual role of kinetic and diffusion-controlled processes in the observed electrochemical behavior, offering a deeper understanding of the interaction between copper ions and the ligand. These findings not only advance the current theoretical framework but also propose new methodologies for optimizing ligand concentration in electrochemical applications, potentially revolutionizing practices in fields such as sensor development and catalytic processes. The novel characterization approach and the comprehensive analysis presented herein lay the groundwork for future studies to explore and exploit these mechanisms further.

5. References

1. L.J.Forney ,C.A. Reddy M Tien mS.D. Aust , (1982)The involvement of hydroxyl radical derived from hydrogen peroxide in lignin degradation by the white rot fungus Phanerochaete chrysosporium., *J. Biol. Chem*. **257** 11455–11462.
2. E.A.Gomaa ,M.M. El-Defraway ,S.Q. Hussien , (2020). Estimation of cyclic voltammetry data for $SrCl_2$, $CaCl_2$ and their interaction with ceftriaxone sodium salt in KNO3 using palladium working electrode, *Eur. J. Adv. Chem. Res.* 1
3. O.J.Fakayode ,T.T.I. Nkambule (2022)Cyclic voltammetric determination of calcium in water in the presence of natural organic matter (humic acid) and Cu (II) at gold electrode's surface, Food Chem. Adv. 1 100012. https://doi.org/10.1016/j.focha.2022.100012.
4. M.V.Sale ,L.B. Reid,L.Cocchi ,A.M.Pagnozzi mS.E. Rose ,J.B., Mattingley, (2017) Brain changes following four weeks of unimanual motor training: Evidence from behavior, neural stimulation, cortical thickness, and functional MRI, Hum. Brain Mapp. **38** 4773–4787.
5. E.W.Moore, (1970) Ionized calcium in normal serum, ultrafiltrates, and whole blood determined by ion-exchange electrodes, *J. Clin. Invest.* **49** 318–334.
6. E.A.Gomaa ,M.A. Morsi ,A.E. Negm ,Y.A. Sherif, (2017) Cyclic voltammetry of bulk and nano manganese sulfate with Doxorubicin using glassy Carbon electrode, *Int. J. Nano Dimens*. 8 89.
7. M.N.Abd El-Hady ,E.A. Gomaa ,A.G. Al-Harazie , (2019)Cyclic voltammetry of bulk and nano $CdCl_2$ with ceftazidime drug and some DFT calculations, *J. Mol. Liq*. **276** 970–985. https://doi.org/10.1016/j.molliq.2018.10.125
8. G.A.Mabbott , (1983) An introduction to cyclic voltammetry, *J. Chem. Educ*. **60** 697.
9. N.Tokman , (2007)The use of slurry sampling for the determination of manganese and copper in various samples by electrothermal atomic absorption spectrometry, *J. Hazard. Mater*. **143** 87–94.
10. K.Nadeau , Z. Mester, L.Yang , (2018) The direct and accurate determination of major elements Ca, K, Mg and Na in water by HR-ICPMS, Sci. Rep. **8** 1–6.
11. R.Kowalik , (2015) The voltammetric analysis of selenium electrodeposition from H2SeO3 solution on gold electrode, Arch. Metall. Mater. **60** 57–63. https://doi.org/10.1515/amm-2015-0009.
12. M.M.El-Kerdawy ,R.I. El-Bagary ,E.F. Elkady ,A.A. Othman , (2016)

Development and validation of a stability-indicating RP-LC method for the simultaneous determination of otilonium bromide and its expected degradation product in bulk drug and pharmaceutical preparation, *Eur. J. Chem.* **7** 97–101.
13. E.A.Gomaa ,A.Z. El-Sonbati ,M.A. Diab ,M.S. EL-Ghareib ,H.M. Salama, (2020) Cyclic Voltammetry, Kinetics, Thermodynamic and Molecular Docking Parameters for the Interaction of Nickel Chloride with Diphenylthiocarbazone, Open Acad. *J. Adv. Sci. Technol*. **4** 30–44.
14. M.A.F.Othman ,A.A. Othman ,H.M. Zuki, (2016) Dithizone modified silver electrode for the determination of metal ions in aqueous solution, Malaysian *J. Anal. Sci*. **20** 197–204.
15. S.Birghila ,M.M. Bratu ,C. Prajitura ,F.N. Roncea ,T. Negreanu-Pirjol , (2015) Spectrophotometric method for the determination of total proteins in egg white samples, Rev. Chim.(Bucharest). 66 378–381.
16. A.I. Gomaa, E.A. Gomaa, R.R. Zaky, M.N. Abd El-Hady, (2024) Design and Synthesis of Pyridine Bis-Hydrazone Metal Complexes of Co(II), Cu(II), and Hg(II): Spectral, Gaussian, Electrochemical, Biological, Drug-Likeness and Molecular Docking Investigations, Inorg. Chem. Commun. 162 112188.
17. A.A.Olajire ,F.E., Imeokparia , (2001)Water quality assessment of Osun River: studies on inorganic nutrients, Environ. Monit. Assess. **69** 17–28.
18. R.Gruden ,A.Buchholz ,O. Kanoun, (2014)Electrochemical analysis of water and suds by impedance spectroscopy and cyclic voltammetry, *J. Sensors Sens. Syst*. **3** 133–140.
19. A.F.El-Baz ,H.M., Abbas, (2017)Isolation and identification of an endophytic fungus from ficus elastica decora and investigation of the antioxidant and antifungal bioactivities of its fermentation extract, *Menoufia J. Agric. Biotechnol*. **2** 81–85.
20 Anwer G. Al-Harazie , Esam A. Gomaa , Rania R. Zaky , Mahmoud N. Abd El-Hady, (2024) Cyclic voltammetry studies of malonamide hydrazone derivative and its electrochemical effect on $CdCl_2$, Electrochimica Acta **476** 143690 https://doi.org/10.1016/j.electacta.2023.143690
21. A.Mohamed ,S. Yousef ,W.S. Nasser ,T.A. Osman ,A. Knebel ,E.P. Sánchez ,T. Hashem, (2020) Rapid photocatalytic degradation of phenol from water using composite nanofibers under UV, Environ. Sci. Eur. **32** 1–8.
22 D.A.El-Kot ,E.A. Gomaa ,A.H. El-Askalany ,R.R. Zaky ,M.N. Abd El-Hady,, (2023) Design of a novel -NOON- tetradentate Schiff-base scaffold supported by α-tetralone and benzothiazole moieties with its Cu^{2+}, Co^{2+}, and Cd^{2+} chelates, *J. Mol. Struct*. 134901.
23. A.S. Nageeb, M.A. Morsi, E.A. Gomaa, M.M. Hammouda, R.R. Zaky, Comparison on biological inspection, optimization, (2024) cyclic voltammetry, and molecular docking evaluation of novel bivalent transition metal chelates of Schiff Base pincer ligand, *J. Mol. Struct*. 1300 137281.
24. .J.M.SAlmeida ,R.M. Dornellas ,S., Yotsumoto-Neto .M. Ghisi ,j.g.c. Furtado ,e.p. Marques ,r.q. Aucélio ,A.L.P. Marques, (2014) A simple electroanalytical procedure for the determination of calcium in biodiesel, Fuel. 115 658–665. https://doi.org/10.1016/j.fuel.2013.07.088.
25. E.A.Gomaa ,M.A. Tahoon,A. Negm, Aqueous micro-solvation of Li+ ions: (2017)Thermodynamics and energetic studies of Li^{+}-(H_2O) n (n= 1--6) structures, *J. Mol. Liq.* **241** 595–602.
26 E.A.Gomaa ,R.R. Zaky ,A. Shokr, (2017)Estimated the physical parameters of lanthanum chloride in water-N, N-dimethyl formamide mixtures using different techniques, *J. Mol. Liq.* **242** 913–918.
27. E.A.Gomaa ,M.H. Mahmoud ,M.G. Mousa ,E.M. El-Dahshan , (2018) Cyclic voltammetry for the interaction between bismuth nitrate and methyl red in potassium nitrate solutions, Chem. Methodol. **3** 1–11.

28 Mohamed Fathi , Esam A.Gomaa, Shereen Salem ,Hamada, Killa ,Hamada M., ,Ayman A. Gouda andAbdel Hamid Farouk, (2023) Parameters for the concductometric association for lump and nano CoSO4.7H2O in the presence and absence of fuchsin acid in water at different temperatures, Bull. Chem. Soc. Ethiop., , **37**(M3), 789-804.

29 J.Nakanishi ,I. Kuramoto ,J. Baba ,K. Ogawa ,Y. Yoshikawa ,H. Ishiguro , (2020) Continuous Hospitality with Social Robots at a hotel, SN Appl. Sci. **2** 1–13.

30 E.M.AbouElleef ,M.N. Abd El-Hady ,E.A. Gomaa ,A.G.Al-Harazie , (2021) Conductometric association parameters for CdBr2 in the presence and absence of Ceftazidime in water and 30% ethanol--water mixtures, *J. Chem. Eng. Data.* **66** 878–889.

31. F.J.R.Rossotti ,H. Rossotti , (1961).The determination of stability constants: and other equilibrium constants in solution,

32. M.D.Murray ,B.Loos ,W. Tu ,G.J. Eckert X-H. Zhou ,W.M., Tierney , (1998), Effects of computer-based prescribing on pharmacist work patterns, *J. Am. Med. Informatics Assoc.* **5** 546–553.

33. A.A.Sharfalddin A.H., Emwas ,M. Jaremko ,M.A. Hussien, (2021) Synthesis and theoretical calculations of metal-antibiotic chelation with thiamphenicol: in vitro DNA and HSA binding, molecular docking, and cytotoxicity studies, *New J. Chem*. **45** 9598–9613.

34. B.A.Babgi ,N.A. Alzaidi ,J.H. Alsayari ,A.-H, Emwas ,M. Jaremko M.,M.H. Abdellattif ,M. Aljahdali .M.A. Hussien (2022) Synthesis, HSA-Binding and Anticancer Properties of [Cu2 (-dppm) 2 (N^ N) 2] 2+, *J. Inorg. Organomet. Polym. Mater*. **32** 4005–4013.

35. N.Daud ,N.A. Yusof S.M..M. Nor . (2013) Electrochemical characteristic of biotinyl somatostatin-14/Nafion modified gold electrode in development of sensor for determination of Hg (II), *Int. J. Electrochem. Sci.* **8** 10086–10099.

36 Peter Agbo, and Nemanja Danilovic, (2019) ,An Algorithm for the Extraction of Tafel Slopes,T*he Journal of Physical Chemistry C*, 1-31, DOI: 10.1021/acs.jpcc.9b06820

37 Anwer G. Al-Harazie, E.A. Gomaa, R.R. Zaky, M.N. Abd El-Hady, (2023) Spectroscopic characterization, cyclic voltammetry, biological investigations, MOE, and Gaussian calculations of VO(II), Cu(II), and Cd(II) heteroleptic complexes, acs omega. **8** 13605–13625. https://doi.org/10.1016/j.electacta.2023.143690 .